

Article type: A-Regular research paper

Optical and Electrophysical Properties of the Germanium Oxynitride-Semiconductor Structure

I. Nakhutsrishvili (1), Z. Adamia (2)

(1) Department of Optically Controlled Anisotropic Systems, Institute of Cybernetics, Georgian Technical University, Georgia, ic@cybernet.ge

(2) Department of Engineering School of Science and Technology, The University of Georgia, info@ug.edu.ge

Corresponding author : zurab.adamia@gmail.com

RECEIVED: 15 February 2025 / RECEIVED IN FINAL FORM: 08 May, 2025 / ACCEPTED: 9 May, 2025

Abstract: The paper studies the optical and electrophysical characteristics of dielectric films of germanium oxynitride obtained by nitridation of single-crystalline germanium with humid ammonia and deposition of reaction products on semiconductor substrates. These films create a high-quality interface with silicon and indium phosphide.

Keywords : SEMICONDUCTORS, GERMANIUM OXYNITRIDE, OPTICAL PROPERTIES, ELECTROPHYSICAL PROPERTIES

I. Introduction

MIS (metal-insulator-semiconductor) structures with a dielectric layer of germanium oxynitride have been studied both previously and currently [1-6]. Earlier than oxynitride, germanium nitride films were studied [7-24]. (It should be considered that they were oxynitrides as well - this is indicated only in some of cited works.)

Films of germanium nitride and oxynitride have become widely used in semiconductor compounds and integrated circuits, since traditional dielectric films (SiO_2 , Si_3N_4 , Al_2O_3 etc.) no longer met the requirements for increasing the speed of these structures and were incapable of creating a sufficiently high-quality interface with semiconductors, in particular with $\text{A}^{\text{III}}\text{B}^{\text{V}}$ semiconductor compounds (GaAs, GaP, GaSb, InSb, InP etc.).

Nitridation of the surface of single-crystalline germanium with ammonia [1, 8 -10] is one of the methods for obtaining its nitride and oxynitride. These are: obtaining a Ge_xON_z film by magnetron sputtering [6], interaction of ammonia with halogen compounds of germanium (GeI_4 , GeCl_4) [10-13, 15], interaction of monogermane (GeH_4) and hydrazine (N_2H_4) [15], nitridation of germanium with hydrazine vapors [16, 18, 19, 20], reactive sputtering of germanium in nitrogen and argon environment [18], interaction of tetraethylgermanium ($(\text{CH}_3\text{CH}_2)_4\text{Ge}$) and hydrazine [21], evaporation of commercial germanium nitride in vacuum [22], nitridation of evaporated germanium in a high-frequency glow discharge of nitrogen [23], interaction of monogermane with hydrazine under high-frequency heating [24].

This article provides a more detailed examination of the optical and electrophysical characteristics of germanium oxynitride films obtained by nitridation of single-crystalline germanium with humid ammonia and depositing the reaction products on semiconductor substrates.

II. Experimental

The studied samples were obtained according to the method described in [25]. Electronic absorption spectra were recorded on a quartz spectrophotometer SF-26-A. Volt-Ampere characteristics were recorded on direct current using an electrometric amplifier U 5 - 6 (measurement limits 10^{-6} - 10^{-15} A). The current through the sample was determined by the voltage drop across the reference resistance. The voltage was measured using a V - 7 - 13 voltmeter. The Volt-Farad characteristics were recorded using the IPPM - 2 setups. The measurements were performed on a sinusoidal signal with an amplitude of 20 mV, a frequency of 1 MHz, and a constant offset. A two-coordinate recorder PDS -0.21 - M was used as a recording device. To study the electrophysical parameters, metal electrodes were applied to the film-substrate structure. Aluminum was used as an ohmic contact: Al wire was evaporated from a tungsten evaporator in a UVN-62-P-1 vacuum unit. The electrodes on the films were formed in the form of washers with a diameter of 0.5 mm, applied through a metal mask. In the case of a Si substrate, a continuous Al layer was deposited on the back side, and in the case of an InP substrate, an InGa alloy was used.

III. Results and Discussion

III. 1. Optical characteristics of $\text{Ge}_x\text{O}_y\text{N}_z$ films

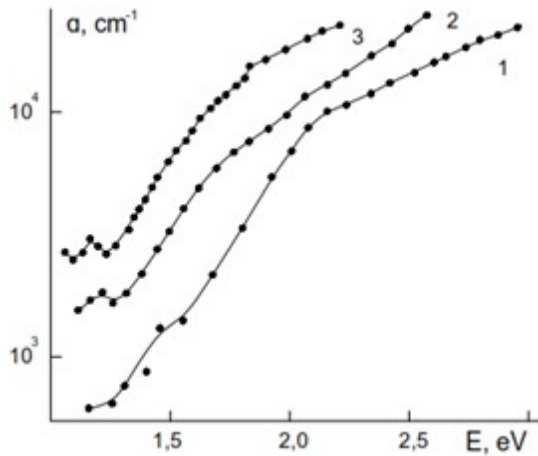
Fig. 1(a) shows the dependence of the absorption coefficient (α) on the energy of photons ($E=h\nu$) for films obtained in different technological modes (temperature of nitridation of germanium: 600, 700 and 800°C).

It should be noted that, despite the similarity of these spectra with the spectra of amorphous elementary semiconductors (C, Si, Ge), they are characterized by somewhat elevated values of α below the fundamental absorption edge, which is determined by the degree of disorder of the amorphous network of the material. The dependence of α on E is divided into three characteristic regions:

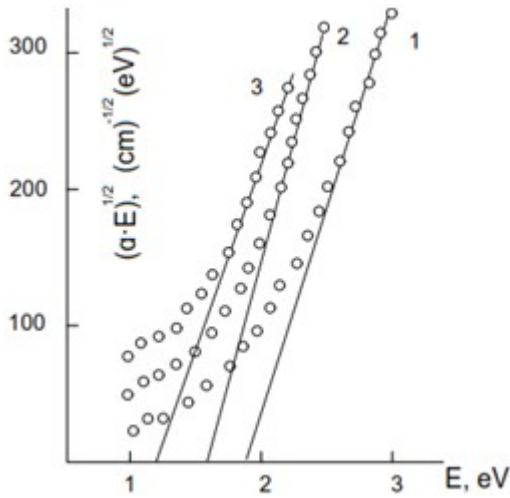
1) region of strong absorption ($\alpha > 10^4 \text{ cm}^{-1}$), which corresponds to interband transitions [26-28] and is described by the equation $E = B \cdot (E - E_{\text{opt}})^2$, where B is a coefficient inversely proportional to the density of states near the conduction band and valence band, and E_{opt} is the optical width of the forbidden band. The value of the coefficient B corresponds to the square of the slope (\tan) of the dependence of the absorption coefficient on the photon energy in the coordinates in coordinates E , $(\alpha E)^{1/2}$ (Fig. 1b). For the considered temperatures of film production, these values are $9.7 \cdot 10^4$, $1.24 \cdot 10^5$ and $7.1 \cdot 10^4 \text{ eV} \cdot \text{cm}^{-1}$, respectively. For comparison, we indicate that in amorphous hydrogenated silicon $B = 4.5 \cdot 10^5 \text{ eV} \cdot \text{cm}^{-1}$ [29]. The comparatively low values of B in our samples can be associated with a high density of states near the edges of the allowed bands. From this point of view, the most favorable temperature for film production is 700°C.

2) region of exponential dependence of α on E , called the Urbach's edge [30, 31] and which is described by the equation $\alpha = \alpha_0 \exp(E/E_0)$, where α_0 is the pre-exponent, E_0 is the Urbach's energy. E_0 can be determined by linearization of the given equation in $\ln \alpha$ - E coordinates (Fig. 1 c, its value corresponds to the cotangent of the slope). The values of Urbach's energy for the considered modes of obtaining germanium oxynitride films are 0.38, 0.35, and 0.29 eV, respectively. The presence of the Urbach's "tail of states" is associated with defects caused by the violation of the long-range ordering of the structure in amorphous materials [32, 33]. A decrease of E_0 with an increase of the film production temperature indicates relaxation of the structural network, which causes a decrease of the absorption caused by defects [34].

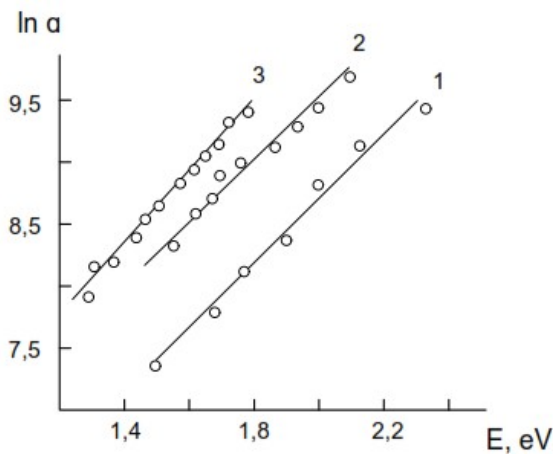
3) region characterized by the appearance of tails of the density of states caused by dangling bonds. This effect is associated with additional absorption at $\alpha < 10^3 \text{ cm}^{-1}$ [35]. In this region, the dependence of α on E is weaker than exponential.



(a)



(b)



(c)

Figure 1: dependence of the absorption coefficient of the oxynitride film on the photon energy.

Electronic absorption spectra of oxynitride films obtained by nitridation of germanium at temperatures 600 (1), 700 (2) and 800°C (3) in coordinates: $\alpha - E$ (a), $\alpha E - E$ (b) and $\ln \alpha - E$ (c)

III. 2. Electrophysical characteristics of $\text{Ge}_x\text{O}_y\text{N}_z$ - semiconductor structures

In MIS (metal-insulator-semiconductor) systems, the electrophysical characteristics of the dielectric films are of decisive importance. Let us consider the systems germanium oxynitride - silicon and germanium oxynitride - indium phosphide.

III. 2. 1. Electrophysical characteristics of $\text{Ge}_x\text{O}_y\text{N}_z$ - Si structure

For structures $\text{Ge}_x\text{O}_y\text{N}_z - \text{Si}$, volt-ampere (UA) characteristics were recorded in the region of both small ($4 \cdot 10^3$ V/cm) and medium ($4 \cdot 10^3 - 6 \cdot 10^4$ V/cm) field strengths. Typical UA characteristics are shown in Fig. 2.

As can be seen from Fig. 2a, Ohm's law is fulfilled in the region of small fields. Only the slope and length of these sections change depending on the temperature of the film preparation. It was previously established that a high-resistance transition layer exists at the amorphous film-semiconductor interface. Its thickness and, therefore, resistance are determined by the conditions of film preparation [36]. Our data probably indicate that increasing the film formation temperature results of a decrease of thickness of the transition layer, which results a corresponding increase of the slope of the U-A characteristics.

In the region of average fields, a superlinear increase in current is observed. In this case, the U-A characteristics are expressed by straight lines in the coordinates $\log I - U^{1/2}$ (Fig. 2b). This may be due to the Poole-Frenkel mechanism, in which field ionization from traps occurs [37, 38].

The conductivity of the obtained structures was measured on direct current with heating of the samples in the range from room temperature to 300 °C. The change of conductivity has an activation character and is described by the equation $\sigma = \sigma_0 \exp(-E_a/K_B T)$, where σ_0 is pre-exponent, E_a is activation energy of conductivity, K_B is Boltzmann's constant, and T is absolute temperature. For all film production modes, the dependence $\log \sigma - T^{-1}$ is the same and is expressed as a straight line with two slopes (Fig.3).

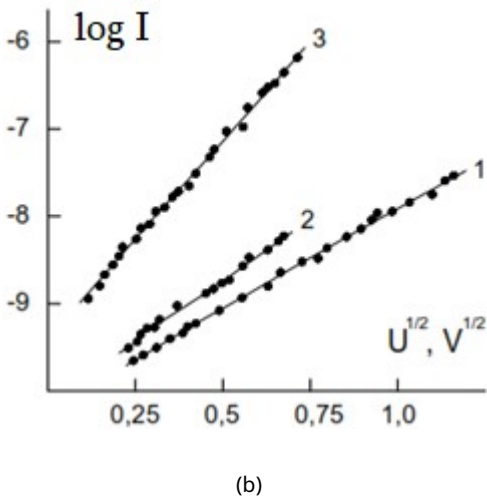
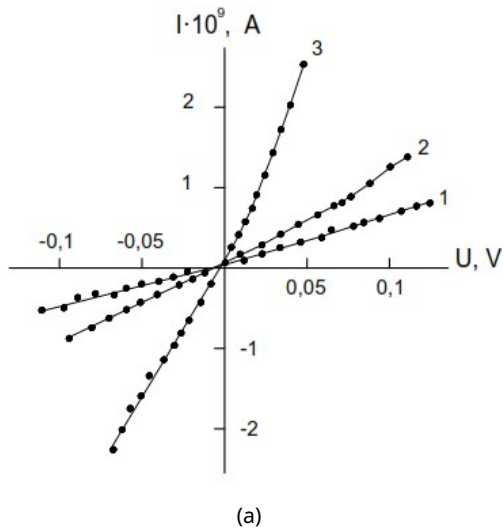


Figure 2: dependence of the current through the oxynitride film on the applied voltage.

Volt-Ampere characteristics of germanium oxynitride films deposited on a silicon substrate, obtained by nitridation of germanium at temperatures 600 (1), 700 (2) and 800°C (3) in coordinates: $I - U$ (a) and $\log \sigma - U^{1/2}$ (b)

It should be noted that the change of slope occurs at approximately the same temperature of heating of the samples (170-190°C). Calculation of the activation energy gives values of 0.26, 0.1 and 0.075 eV for the low-temperature region and 0.75, 0.3 and 0.23 eV for the high-temperature region for films obtained at 600, 700 and 800°C, respectively. To interpret the obtained results, the Mott-Davis model can be used [39]. According to this model, two values of the activation energy of conductivity are associated with the existence of two types of traps (shallow and deep) in the forbidden zone, the ionization of which determines the current flow in the material.

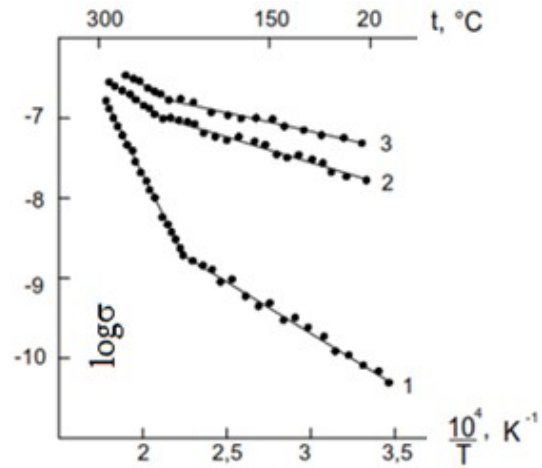


Figure 3: dependence of the conductivity of the oxynitride film on temperature.

Temperature dependences of electrical conductivity of MIS structures based on germanium oxynitride films obtained by nitriding germanium at temperatures 600 (1), 700 (2) and 800°C (3) in Arrhenius coordinates

We investigated the capacitance-voltage (C-U) characteristics of the germanium oxynitride-silicon structure. A typical dependence of the change of the capacitance of the structures on the constant voltage is shown in Fig.4. The C-U dependence is characterized by a hysteresis of 0.5-0.8 eV and a clockwise direction of the loop. This indicates the existence of traps in the material [40, 41].

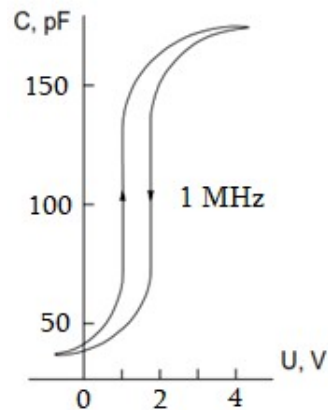


Figure 4: dependence of the capacitance of the MIS structure on the applied voltage.

C-U characteristic of germanium oxynitride-silicon structure

The presence of traps in the volume of the material can be used to store of charge in memory elements [42, 43].

III. 2.2. Electrophysical characteristics of $\text{Ge}_x\text{O}_y\text{N}_z$ - InP structure

Indium phosphide is a promising material among other $\text{A}^{\text{III}}\text{B}^{\text{V}}$ - type semiconductor compounds [44-47]

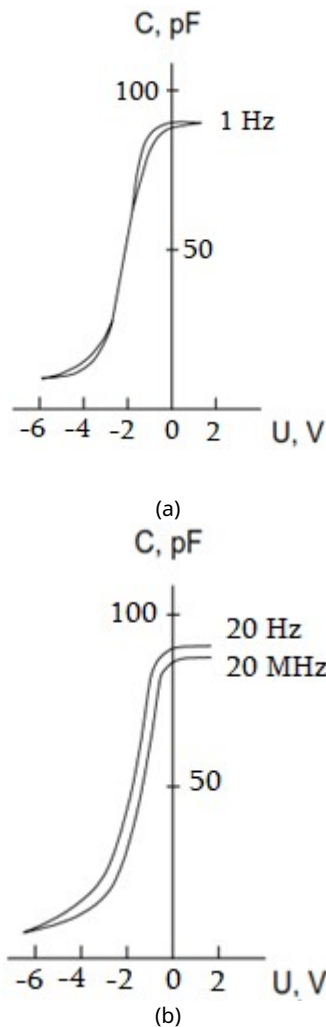


Figure 5: dependence of the capacitance of the MIS structure on the applied voltage.

C-U characteristics of germanium oxynitride-indium phosphide structure (film production temperature 700°C)

The C-U characteristics of $\text{Ge}_x\text{O}_y\text{N}_z$ - InP structure were measured in the frequency range 1Hz (Fig. 5a) and 20 Hz - 20 MHz (Fig. 5b). The figure shows the practical absence of hysteresis in the frequency range under study. It is also evident that the structure has a very low frequency dispersion. These data indicate a low density of surface states, which determines the prospects for using the germanium oxynitride - indium phosphide structure to create MIS devices and integrated circuits.

Conclusion

The optical and electrophysical characteristics of dielectric films of germanium oxynitride - semiconductor systems are studied. Films of germanium oxynitride are obtained by nitriding of single-crystalline germanium with humid ammonia and deposition of reaction products on Si and InP substrates. The dependence of the absorption coefficient on the energy of photons is divided into three characteristic regions: region of strong absorption ($\alpha > 10^4 \text{ cm}^{-1}$), which corresponds to interband transitions, region of exponential dependence of α on E (the Urbach's edge) and region characterized by the appearance of tails of the density of states caused by dangling bonds ($\alpha < 10^3 \text{ cm}^{-1}$). For the mechanism of current flow in films, the Mott-Davis model can be used. The capacitance-voltage characteristics of $\text{Ge}_x\text{O}_y\text{N}_z$ - Si structure have hysteresis. These structures can be used to store of charge in memory elements. The C-U characteristics of the $\text{Ge}_x\text{O}_y\text{N}_z$ - InP structure in the frequency range of 20 Hz - 20 MHz have very low frequency dispersion. This defines the prospect of using the structure for creating MIS devices and integrated circuits.

Appendix - Film preparation

Let us consider in more detail the method for obtaining germanium oxynitride films that we used in [25] and some other works. The nitride samples were obtained by nitriding of single-crystal germanium (n-type conductivity, resistivity $35 \Omega \cdot \text{cm}$, orientation $\{111\}$ or $\{100\}$) in the $\text{NH}_3 + \text{H}_2\text{O}$ medium at 640-840°C under static vacuum conditions. Germanium plates were etched in a liquid etchant CP-4A ($\text{HF} : \text{HNO}_3 : \text{CH}_3\text{COOH} = 1:15:1$) for 5min and washed in double-distilled water, followed by drying. Commercial ammonia (99.6% NH_3 , 0.2-0.4% H_2O) was purified both by the standard method (passing over CaO and NaOH absorbers) also by freezing in a mixture of liquid nitrogen and alcohol at a temperature of -30°C (freezing temperature of ammonia is -33.4°C). The pressure of ammonia was $2 \cdot 10^3 \text{ Pa}$. The nitride samples were synthesized under the following conditions: $P \equiv P_{\text{H}_2\text{O}} / P_{\text{NH}_3} \cong (2-4) \%$. The duration of the reaction was 2 hours. The obtained nitride was analyzed by X-ray (diffractometer

HZG-A, CuK_α radiation) and Auger electron spectroscopy (spectrometer LAS-2000).

The formation of germanium nitride in humid ammonia is accompanied by its simultaneous evaporation. Water vapor forms volatile germanium monoxide, which evaporates completely and does not remain in the surface product. Simultaneous evaporation of germanium nitride and oxide results in the deposition of a film of germanium oxynitride in the "cold" (300-350 °C) zone of the reactor.

It should be specially noted that germanium monoxide disproportionates when deposited on a substrate: $2\text{GeO}=\text{Ge}+\text{GeO}_2$. As a result, excess germanium appears in the film. And this explains a certain difference between the above-considered properties of $\text{Ge}_x\text{O}_y\text{N}_z$ and the properties of stoichiometric films of germanium nitride and oxynitride.

REFERENCES

1. A.V.Rzhanov and I.G.Neizvestny. *Thin Solid Films*, **vol. 58**, p 37 (1979)
2. B.C.Hsu, Ch.H.Lin, P.-S.Kuo et al., *Electron Device Lett.*, **vol. 25**, p 544 (2004)
3. Y.Fukuda, K.Kato, T.Toyota et al., *Jap. Applied Physics*, **vol. 45**, p 7351 (2006)
4. K.Kutsuki, G.Okamoto, T.Hosoi et al., *Appl. Phys. Lett.*, **vol. 95**, p 022102 (2009)
5. J.Wang, Y.Asakura and Sh.Yin, *Hazardous Materials*, **vol. 396**, 122709 (2020)
6. Sh.J.Du, X.-X.Li, Y.Tian et al. *Nuclear Sci. and Techniques*, **vol. 35**, p 45 (2024)
7. V.Synorov, A.Kuznetsov and N.Aleinikov. *High. Educ. Inst.-Phys.*, **vol. 3**, p 7 (1967)
8. N.Aleinikov, A.Barabashina and V.Synorov. *Inorg. Chem.*, **vol.12**, p 3387 (1967)
9. Y.Igarashi, K.Kurudama and T.Niimi. *Jap. Applied Physics*, **vol. 7**, p 300 (1968)
10. H. Nagai and T.Niimi. *Electrochem. Soc.*, **vol. 115**, p 671 (1968)
11. L. Vasilyeva, T.Kovalevskaya et al. *Inorg. Materials*, **vol.5**, p 1537 (1969)
12. T.Yashiro. *Jap. Applied Physics*, **vol. 10**, p 1961 (1971)
13. T. Yashiro. *Electrochemical Soc.*, **vol. 199**, p 780 (1972)
14. V. Myakinenkov, V.Nogin, B.Anokhin et al. *Semicond. Dev.*, **vol. 79**, p (1973)
15. G. Shanable, W.Kern and R.Comizzoli. *Electrochem. Soc.*, **122**, p 1092 (1975)
16. G. Bagratishvili, R.Dzhanelidze et al. *Phys. Stat. Sol.*, **vol. 36**, p 73 (1976)
17. G. Bagratishvili, R.Dzhanelidze et al. *Thin Solid Films*, **vol. 56**, p 209 (1979)
18. G.Bagratishvili, R.Dzhanelidze et al. *Phis. Stat. Sol.*, **vol. 65**, p 701 (1981)
19. I.Nakhutsrishvili. *Oriental J. Chem.*, **vol. 36**, p 850 (2020)
20. I.Nakhutsrishvili, R.Kokhraidze et al. *Oriental J. Chem.*, **vol. 38**, p 211 (2022)
21. L.A.Ivanyutin, N.N.Dyachkova and B.I.Kozyrkin. *Electronic Eng.*, **vol. 6**, p 105(1976)
22. B.Bayraktaroglu, R.Johnson et al. Nort Carolina Univ. Conf., June 18, p 207 (1980)
23. K.Pande, M.Chen and M.Yousuf. *Solid State Electronics*, **vol. 24**, p 1107 (1981)
24. K.Pande. *Solid State Electronics*, 1982, **vol. 25**, p 145 (1982)
25. Z.Vardosanidze, I.Nakhutsrishvili et al. *Coating Sci. Technol.*, **vol. 11**, p 1 (2024)
26. J.Toudert and R.Serna. *Opt. Materials Express*, **vol. 7**, p 2299 (2017)
27. A.I.Ekimov and V.I.Safarov. *JETP Letters*, **vol. 118**, p S38 (2023)
28. K.Jaya Bala, A.J.Peter and Ch.W.Lee. *Optik*, **vol. 183**, p 1106 (2019)
29. Y.Sakata, J.Hayashi, M.Yamaraka et al. *Appl. Phys.*, **vol. 52**, p 4334 (1981)
30. E.Ugur, M.Ledinský, T.Allen et al. *Phys. Chem. Lett.*, **vol. 13**, p 7702 (2022)

31. J.Holovský, K.Ridzoňová, A.Amalathas et al. *Energy Lett.*, **vol. 8**, p 3221 (2023)
32. L.Wang, B.Liu, H.Li et al. *Science*, **vol. 337**, p 825 (2012)
33. Ch.An, Y.Zhou, Ch.Chen et al. *Adv. Materials*, **vol. 32**, 2002352 (2020)
34. Physics of hydrogenated amorphous silicon. Ed. J.Joannopoulos, p 290 (1984)
35. F.Martinez-Viviente, A.del Prado, I.Mártil et al. *Appl. Phys.*, **vol. 84**, p 149 (2000)
36. D. G. Ast, M. H. Brodsky, *Non-Crystalline Solids*, 1980, 35/36, 611-616.
37. H.Schroeder. *Appl. Phys.*, **vol. 117**, p 215103 (2015)
38. P.Mainali, P.Wagle, Ch.McPherson and D.McIlroy. *Science*, **vol. 5**, p 3 (2023)
39. N.F. Mott and E.A Davis. Clarendon-Press, Oxford, p 437 (1971)
40. S.Kim, H.Yoo and J.Choi. *Sensors*, **vol. 23**, p 2265 (2023)
41. P.Roy, S.Kunwar, D.Zhang et al. *Adv. Electron. Materials*, **vol. 8**, p 2101392 (2022)
42. D.Di Maria, D.Dong and C.Faicoly. *Appl. Phys.*, **vol. 54**, p 580 (1983)
43. D.Jeltsema, A.Doria-Cerezo. Proceedings of the IEEE 100, p 1928 (2012)
44. A.Yoshikawa and Y.Sakai. *Solid-State Electronics*, **vol. 20**, p 133 (1977)
45. M.Bettini, K.Bachmann, E.Buehler et al., *Appl. Phys.*, **vol. 48**, p 1603 (1977)
46. M.Purica, E.Budianu, E.Rusu and P.Arbadji. *Thin Sol. Films*, **vol. 511**, p 468 (2006)
47. K.Schulte, J.Daniel, D.Friedman et al. *Adv. Ener. Mater vol. 14*, p 2303367 (2024)